USING LIDAR TO ESTIMATE LADDER FUEL DENSITY IN FORESTED AREAS

Heather E. Casper and Keith T. Weber, Idaho State University GIS Training and Research Center, Pocatello, ID 83209

ABSTRACT
A trend of increasing wildfire frequency has necessitated the development of methods to identify forested areas with heightened fire susceptibility. One specific concern in forested areas is susceptibility to canopy fires due to the presence of ladder fuels. Fuel reduction treatments that target areas where ladder fuels are present are effective at mitigating canopy fires, but it is difficult to identify where ladder fuels exist within large forests. Past studies have demonstrated lidar (Light Detection and Ranging) technology can be used to detect the presence of ladder fuels. This study began with a literature review investigating current lidar applications for ladder fuel identification and subsequently led to the development of a model that quantifies ladder fuel density in forested areas. The model output is a raster image that can be used by land managers to help prioritize fuel load/ladder fuel reduction treatments. The accuracy of the model was field validated in the summer of 2025, demonstrating sites with predicted low estimated ladder fuel density (20%) do indeed exhibit low ladder fuel abundance in the field. Likewise, sites predicted as having high estimated ladder fuel density (66%) exhibited high ladder fuel abundance in the field.

KEYWORDS
lidar; remote sensing; hazard mitigation; wildfires; fire management; forest management; forest density; ladder fuels; geospatial model

INTRODUCTION
Across the globe, the frequency of occurrence and severity of weather conditions suitable for wildfire ignition (fire weather) have increased over the past decade [1]. Concomitantly, there has also been an increase in both the number and size of wildfires [2]. These wildfires have caused damage to human life and property and have resulted in substantial economic losses [3]. Regardless of the underlying causes for the increase in wildfires, there is a need to develop effective methods to mitigate the disturbance caused by these fires.

Land managers frequently use fuel load reduction treatments to mitigate wildfire hazard [4]. Fuel load reduction consists of the manual or mechanical clearing of surface fuels (e.g., shrubs and low growing plants) and ladder fuels. Ladder fuels are flammable biomass located between low surface fuels and higher canopy fuels. When a wildfire burns only surface fuels, the fire can be managed more rapidly and effectively. However, if ladder fuels are present, fires can readily spread into the tree canopy allowing the fire to move much more quickly and making it more difficult to control [4]. Ladder fuel reduction treatments are effective in mitigating wildfire hazard because the disruption in the spatial and vertical continuity of readily available fuels a wildfire could consume results in fewer canopy fires [5].

To apply ladder fuel reduction efforts effectively, land managers need to know where in a forest ladder fuels exist in greatest abundance. Menning and Stephens [6] addressed the issue of assessing ladder fuel hazard in forests by creating an approach known as the ladder fuel hazard assessment (LaFHA). The LaFHA is a workflow that uses both physical measurements and visual observations of forest attributes to identify the appropriate category of risk into which an area of interest (AOI) falls. This analysis relies upon subjective visual observations, and Menning and Stephens reported that results often varied between observers. In addition, the LaFHA method requires time-consuming, manual field measurements that may not be economically feasible when large AOI's require assessment [7]. Manual ladder fuel hazard assessments are ineffective and outdated which has necessitated the development of new methodologies to accomplish this.

In recent years, lidar (Light Detection and Ranging) technology has proven effective in creating more consistent and reliable methods of assessing ladder fuel hazard by quantifying the abundance of ladder fuels in a forested region [8]. Due to the ability of lidar pulses to penetrate through the forest canopy, specific metrics can be applied to lidar point cloud (LPC) returns that visualize and quantify the density of understory vegetation [9]. Kramer et al. [10] further developed these metrics so that surface fuels were removed and only intermediate ladder fuel data remain. As a result, Kramer's team was able to develop an equation whose independent variables are lidar-derived metrics that can be reliably used to quantify the density of ladder fuels in a forest [11, 12]. Kramer's equation was derived primarily for use in ladder fuel estimations in mixed-conifer forests like the Klamath Mountains of northern California, and use in differing forest conditions should be exercised with caution. However, Kramer and her team suggest that this methodology can establish an effective baseline surrogate for ladder fuel hazard assessment for land managers across their management areas [11].

Implementing Kramer's equation, however, requires a comprehensive understanding of lidar technologies. Processing LPC data for use in the equation requires the user to derive several specific metrics from the data. Deriving these metrics requires finely tuned use of geoprocessing tools and of python scripting by a technician that is versed in Geographic Information Systems (GIS) and in the workings of lidar data. If a trained GIS expert is not available to perform these calculations, the benefit from Kramer's work is extremely limited. The high level of expertise needed to derive these metrics and use this equation places constraints on its widespread application and reduces the overall accessibility of the technology.

Additionally, processing data from Kramer's equation is labor-intensive and time consuming because the same metrics need to be individually derived from each LPC tile in the input data. This results in long processing times and high room for user error during data entry stages, especially for large datasets with a large number of input LPC tiles.

To address these issues, we used Kramer's equation to create a functional and accessible model for estimating ladder fuel density, the ladder fuel calculation model (LFCM). The output of the LFCM is a single raster layer that displays the estimated density of ladder fuels within the forested regions of an AOI. The LFCM is globally scalable wherever LPC data can be sourced. Further, any number of inputs LPC tiles can be analyzed as one in a project, meaning any size data set can be analyzed by the LFCM. Ultimately, the ladder fuel density layer generated by the LFCM can be widely used by land managers to help prioritize areas for fuel load reduction treatment, aiding in the prevention of canopy fires and thereby the mitigation of wildfires.

When compared to earlier methodologies such as the LaFHA, the LFCM eliminates almost all user subjectivity because it is not dependent on manmade field observations. Further, the automation of the ladder fuel calculation process with the LFCM minimizes the amount of human involvement needed to employ Kramer’s effective methodology which reduces the time and resources spent in the calculation process as well as reduces room for human error.

The LFCM condenses a labor-intensive, complicated process into five easy-to-use geoprocessing tools with associated tutorial documentation that clearly explains how to operate each tool. Only minimal training, which is provided in the tutorial documentation, is needed to operate the model, and the user does not need to be a GIS or lidar expert to do so. The LFCM is easier to use and produces more consistent results than previous applications of Kramer’s methodology. For these reasons, and also because the model is freely available for public download and use (see data availability statement), the LFCM improves the visibility, usability, and accessibility of Kramer’s research and has the potential to be a powerful tool for land managers.

To investigate the accuracy of LFCM in the field, we completed the model for an AOI and applied a hot-spot analysis to the resulting ladder fuel density raster layer to identify sites of extremely low ladder fuel density and extremely high ladder fuel density. We visited these sites and made observations of the abundance of the ladder fuels present which were examined against the results of the LFCM.

MATERIALS AND METHODS

Model Design

This study applied the methodology outlined by Kramer et al. [11] to build a model to estimate ladder fuel density. We chose this methodology because the results from Kramer’s method aligned well with observed values and were statistically significant (R^2 =0.73, $P < 0.05$). We used rapid Lasso’s LAStools [13], ArcGIS Pro [14], and Python scripts to create the LFCM, which is a suite of geoprocessing tools that uses either LAS or LAZ file inputs and a polygon feature class of the AOI to create a single output raster estimating the density of ladder fuels found within each forested pixel. The LFCM is composed of five processing steps, each of which performs a specific function in the calculation process (**Figure 1**).

We used ArcGIS Pro's Model Builder functionality to build the first step in the model which normalizes all points in the input LPC data. Normalization is the process where the software -in this case the lasheight function of LAStools- assigns the elevation value of all LPC ground points to 0. All other points are assigned an elevation value relative to their height above ground [15]. We chose to modify Kramer's methodology and use normalized LPC data rather than raw LPC data as input for the model because normalizing LPC data eliminates the negative effects of variable point density [16]. To execute this step of the model, the user must provide the full path file name of the folder containing the input LPC data. An optional wildcard character can be used here to further specify which LPC files the tool accepts from the folder. When run, this tool iteratively normalizes each of the input LPC files. Each resulting normalized LPC file is automatically stored in a preexisting folder within the project titled "02_Normalized_LAS."

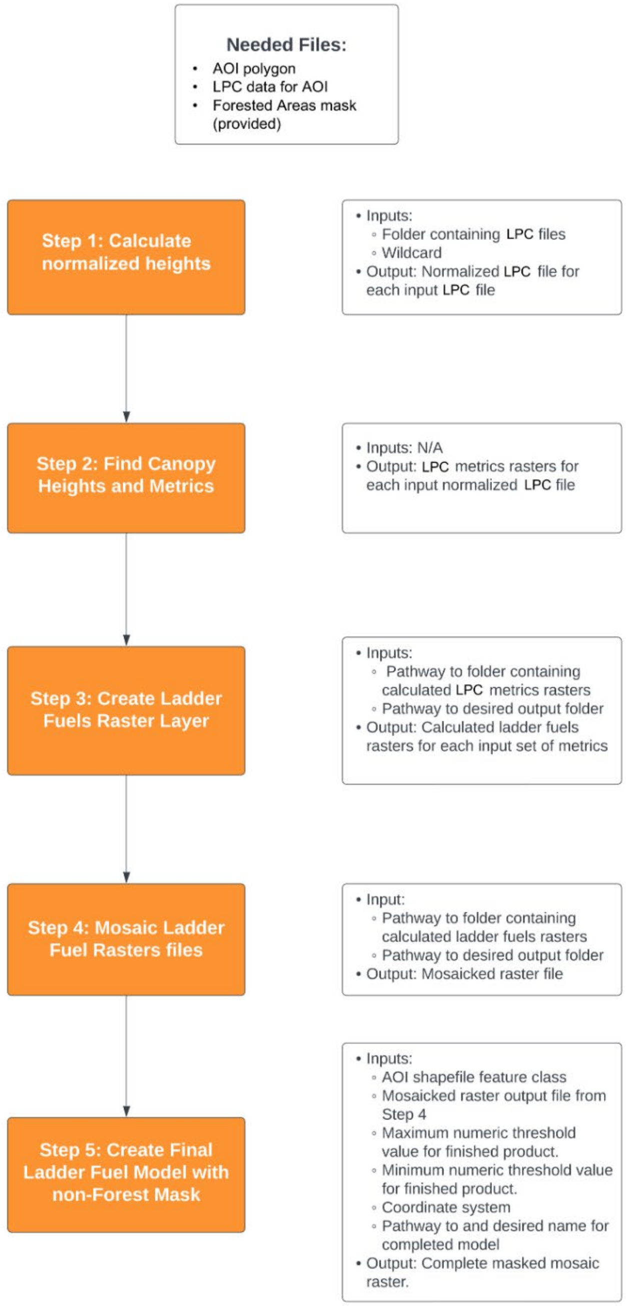

Figure 1. The five processing steps for the ladder fuel calculation model (LFCM). The model takes input lidar point cloud (LPC) file(s) and a polygon shapefile of the area of interest (AOI) and creates a single output raster estimating the density of ladder fuel

The second step of the LFCM uses Model Builder to derive specific metrics from each of the normalized LPC files. These metrics (COV1_8, STD, and FCOV8_16) are derived using the lascanopy functionality of LAStools and are needed in step three of the model. The specific metrics were identified by Kramer et al. [11] and used in their approach to ladder fuel density modeling. The variable COV1_8 is the percent of all classified lidar returns between 1 and 8 meters, STD is the standard deviation of lidar point heights above two meters, and FCOV8_16 is the percent of first returns between 8 and 16 meters. This step automatically draws input from the "02_Normalized_LAS" file folder and requires no user input. When run, this tool iteratively derives the needed metrics from each of the input normalized LPC files. The resulting metric files for each normalized LPC file are automatically stored in a preexisting folder within the project titled "03_LadderFuel_Metrics." It is of note that the metrics calculated in this step of the LFCM are, in their current state, translated straight from Kramer's equation [11]. However, these metrics can be manually changed by the user to better reflect the fire behavior patterns of their specific AOI.

In the third step of the LFCM, a python script uses the derived metrics for each LPC as input variables for Equation 1 [11]. This tool generates a single output raster for each input LPC file showing the estimated ladder fuel density within each pixel. To execute this step of the model, the user must provide the full path of the folder containing the derived metric data (e.g. "03_LadderFuel_Metrics") and of the desired folder where calculated ladder fuels rasters should be stored after processing.

In the fourth step of the model, a python script uses ArcGIS Pro's Mosaic to New Raster geoprocessing tool to mosaic all ladder fuel raster layers into a single raster layer which is used as input in the final step of the model. To execute this step of the model, the user must provide the full path of the folder specified in step three containing the ladder fuel rasters and of the desired folder where the complete mosaicked ladder fuel raster file should be stored after processing.

$$\text{LadderFuelCover} = 20.41 + 0.873 \times (\text{COV1\_8}) - 1.73 \times (\text{STD}) - 0.189 \times (\text{FCOV8\_16})$$

Equation 1

Using Model Builder and a series of geoprocessing tools, the final step of the LFCM applies a mask to the output mosaicked ladder fuel raster layer to include results in forested areas only. The forested areas mask is identified by a Boolean raster layer. The data layer already provided with the LFCM is derived from LANDFIRE's Existing Vegetation Type data [17] and can be used for any AOI in the contiguous United States. An alternative source of forested areas may be used as long as the layer is represented as a simple Boolean type where pixels with a value of one indicate a forested area and pixels with a value of zero are non-forested areas. To execute this step of the model, the user must provide the full path to a polygon shapefile of the AOI, the folder containing the mosaicked ladder fuel raster, and to the desired folder where the complete ladder fuel raster file should be stored after processing. This tool additionally allows the user to specify (a) the minimum and maximum percent thresholds to be included in the final raster (typically zero and 100, respectively) and (b) the desired output spatial reference system of the ladder fuel raster.

Study Area and Model Validation

The LFCM was completed for a study area in southeast Idaho. Bannock County (**Figure 2**) covers 771,680 acres of diverse land cover and ownership patterns and was chosen primarily due to close proximity with the research facilities. Determined by the United States Department of Agriculture's (USDA) Forestry Inventory and Analysis (FIA) program, 178,747 acres (24.3%) of the land in Bannock is forested [18]. A polygon shapefile depicting the extent of Bannock County was retrieved [19], and lidar LPC data for Bannock county was downloaded from the Idaho Lidar Consortium.

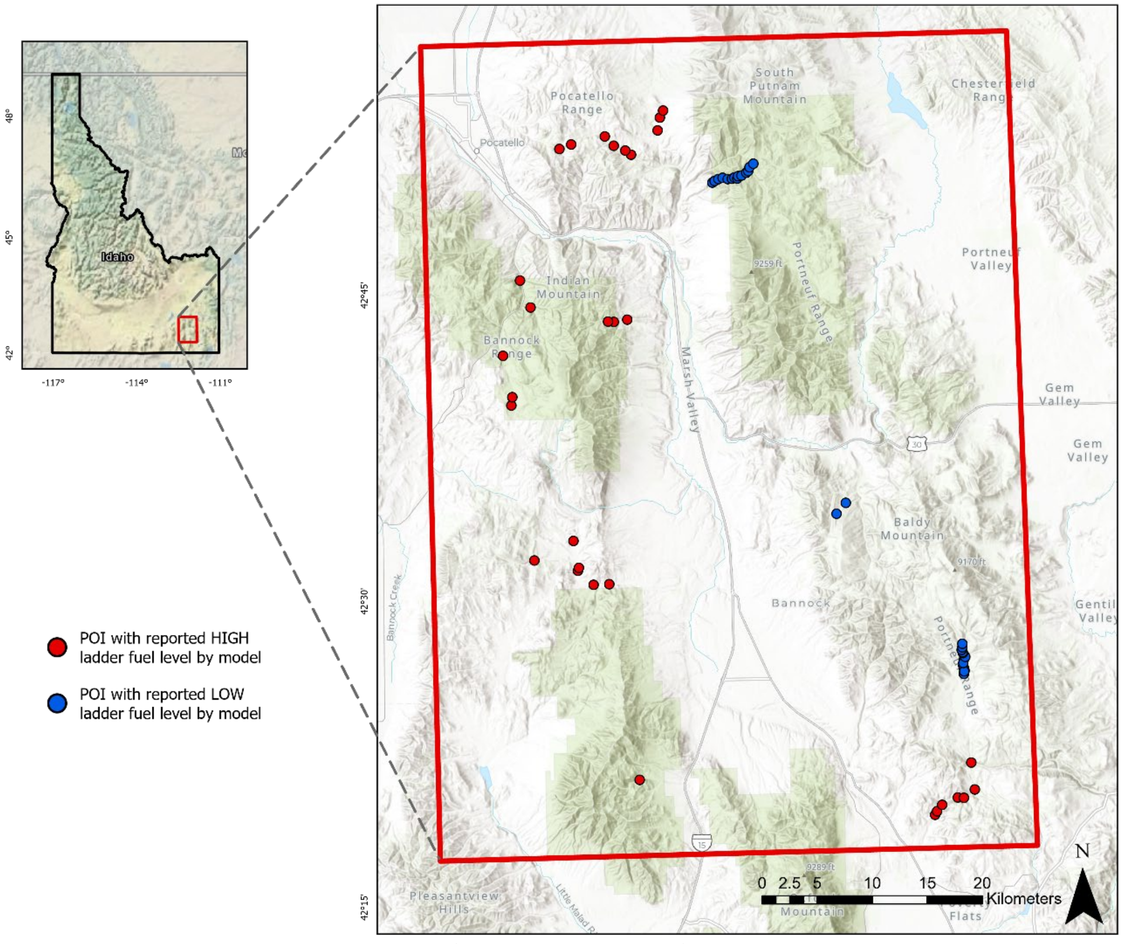

Figure 2. The extent of the study area, Bannock County, Idaho. Points of Interest (POI) with high estimated ladder fuel density are shown in red, and POIs with low estimated ladder fuel density are shown in blue.

These data were a mosaic of several lidar project datasets acquired between 2013 and 2023, sponsored primarily by the Federal Emergency Management Agency (FEMA) and US Geologic Survey (USGS) [20-28]. Metadata for each input lidar project used are shown in **Tables 1-5**. Due to the variations in how the multiple input datasets were collected and processed, there is the potential that heterogeneous point densities and other issues occurred completed output raster. This could potentially lead to sections of the AOI from one input dataset having all higher or all lower values than in another input dataset. Because our study area was large and used LPC data from multiple sources, there is potential for heterogeneous point density issues.

Table 1. Overview of the various sponsors and the date ranges in which data was collected for each of the input lidar datasets used in model validation.

Dataset Name	Sponsor	Date Range
Blackfoot & Portneuf, ID	Boise State Univ.	1-29 Oct 2017; 8 Nov 2017
Franklin Bear, ID	USGS (3DEP)	13-28 Oct 2017; 8 Nov 2017
OLC Snake River	Oregon LiDAR Consortium	22 Apr – 2 Jun 2015
Oxford Slough WPA, ID	USFWS / Aero-Graphics	9 - 12 Nov 2013
Southern ID 06_2018	USGS (3DEP) / Dewberry	Oct 2019 – May 2020
Southern ID 08_2018	USGS (3DEP)	26 Sept 2019 -20 Jun 2020
Southern ID 09_2018	USGS (3DEP) / Dewberry	Sept 2019 – Jun 2020
Southern ID 17_2018	USGS (3DEP) / Dewberry	Sept 2019 - Aug 2020
Southern ID 22_2018	USGS (3DEP) / Dewberry	Oct 2019 – Sept 2020

Note: ID = Idaho; USFWS = U.S. Fish and Wildlife Service; 3DEP = 3D Elevation Program

Table 2. Overview of the various lidar Sensor and aircraft platform specifications used for each of the input lidar datasets used in model validation.

Dataset Name	Sensor Type	Aircraft Platform
Blackfoot & Portneuf, ID	Leica ALS80	Cessna Caravan
Franklin Bear, ID	Leica ALS80; Optech Galaxy	Cessna 208B; Cessna 310
OLC Snake River	Leica ALS70	Cessna Grand Caravan
Oxford Slough WPA, ID	Optech ALTM Orion	Cessna 207 (turbo)
Southern ID 06_2018	Optech Galaxy Prime	Cessna 310; Cessna T206
Southern ID 08_2018	Optech Galaxy; Riegl VQ1560i	Cessna (various)
Southern ID 09_2018	Optech Galaxy Prime	Cessna T-310; Cessna T-206
Southern ID 17_2018	Optech Galaxy; Riegl VQ1560i	Cessna 310, T206, 206
Southern ID 22_2018	Optech Galaxy; Riegl VQ1560ii	Piper Navajo; Cessna 310, T206

Table 3. Overview of lidar acquisition parameters used for each of the input lidar datasets used in model validation.

Dataset Name	Scan Angle (°)	Pulse Ratio (kHz)	Returns per Pulse	Density (pts/m^2)
Blackfoot & Portneuf, ID	±15	313-343	Unlimited	11.43
Franklin Bear, ID	±15-18	340-350	Unlimited; ≤8	11.70
OLC Snake River	±15	198	Single	10.49
Oxford Slough WPA, ID	±15	125	≤4	11.33
Southern ID 06_2018	±15-23	300-650	≤7	7.5-27.8
Southern ID 08_2018	±14-29	300-700	≤7; Unlim.	27-30 (QL1)
Southern ID 09_2018	±14.75	600	≤7	30.4
Southern ID 17_2018	±20-29	300-700	≤7; Unlim.	9.87
Southern ID 22_2018	±20-29	300; 1000	≤15; ≤7	7.73

Note: pts = points; Unlim. = Unlimited. Density values are actual measured values

Table 4. Overview of the lidar data processing software and methods used for each of the input lidar datasets used in model validation.

Dataset Name	Processing Software	RTK	PPK
Blackfoot & Portneuf, ID	POSPac; Terrascan; Waypoint	Yes	Yes
Franklin Bear, ID	POSPac; Terrascan; Waypoint	Yes	Yes
OLC Snake River	QSI proprietary; OPUS GNSS	Yes	Yes
Oxford Slough WPA, ID	POSPac; ALTM-Nav	-	Yes
Southern ID 06_2018	POSPac; Terrascan; LP360	-	PP-RTX
Southern ID 08_2018	POSPac; Terrascan; LP360	-	PP-RTX
Southern ID 09_2018	POSPac; Terrascan; LP360	-	PP-RTX
Southern ID 17_2018	POSPac; Terrascan; RiParam; LP360	-	PP-RTX
Southern ID 22_2018	POSPac; Terrascan; RiParam; LP360	-	PP-RTX

Note: PP-RTX = Trimble Precise Point Real-Time eXtended; RiParam = RiParameter
RTK = Real-time Kinematic correction of GNSS data
PPK = Post-Processed Kinematic correction of GNSS data

Table 5. Overview of the lidar vertical accuracy metrics used for each of the input lidar datasets used in model validation.

Dataset Name	RMSE (cm)	Accuracy @95% (cm)
Blackfoot & Portneuf, ID	3.4	6.7
Franklin Bear, ID	3.4	6.6
OLC Snake River	3.6	7.0
Oxford Slough WPA, ID	2.7 (FVA)	5.1 (FVA)
Southern ID 06_2018	9.7	18.9
Southern ID 08_2018	7.4	14.5
Southern ID 09_2018	3.5	6.81
Southern ID 17_2018	5.6	10.9
Southern ID 022_2018	10.1	19.6

Note: RMSE = Root Mean Square Error; FVA = Fundamental Vertical Accuracy.

Upon running the model with these datasets as inputs, a 1 meter per pixel raster file depicting the estimated density of ladder fuels in the forested regions in Bannock County was produced (**Figure 3**; left). To reduce single pixel "salt and pepper" anomalies a minimum mapping unit of approximately 1 hectare (900 m^2 or 30 meters per pixel) was applied to the output raster ladder fuel model used to identify field sample sites. Sites in the study area with the highest and lowest estimated ladder fuel densities were identified using ArcGIS Pro's Getis-Ord hot spot analysis [29].

Low percent ladder fuel areas were identified to be statistically significant "cold spots" (99% confidence) and represented places where ladder fuel density estimates averaged 20%, as determined by the LFCM. High percent ladder fuel areas were identified to be statistical "hot spots" (99% confidence) and ladder fuel density estimates averaged 66%, as determined by the LFCM. From these data, a map showing 61 field sampling sites located on easily accessible public land were identified, 31 of which were located in high ladder fuel density locations (hot spots) and 30 in low ladder fuel density locations (cold spots) (**Figure 3**; right) was created. A 20-meter buffer was created around each POI using ArcGIS Pro's buffer tool. Using the zonal statistics geoprocessing tool, the mean estimated ladder fuel density for all pixels within each polygon buffer zone were extracted and analyzed for accuracy.

In June 2025, all 61 sites were visited, and *in situ* validation data was recorded for each point of interest (POI) including a unique ID number, dominant tree overstory type (conifer or broadleaf), estimated tree height, the presence or absence of ladder fuels, and observations of site ladder fuel abundance. Observations were recorded over five separate field days using ArcGIS Field Maps software. Three or more site photographs were taken at each POI. The estimated heights of trees were measured using a Nikon Forestry Pro II Rangefinder (average error of ±0.3 meters).

All field data were downloaded to ArcGIS Pro and exported to an Excel spreadsheet for analysis and validation processing.

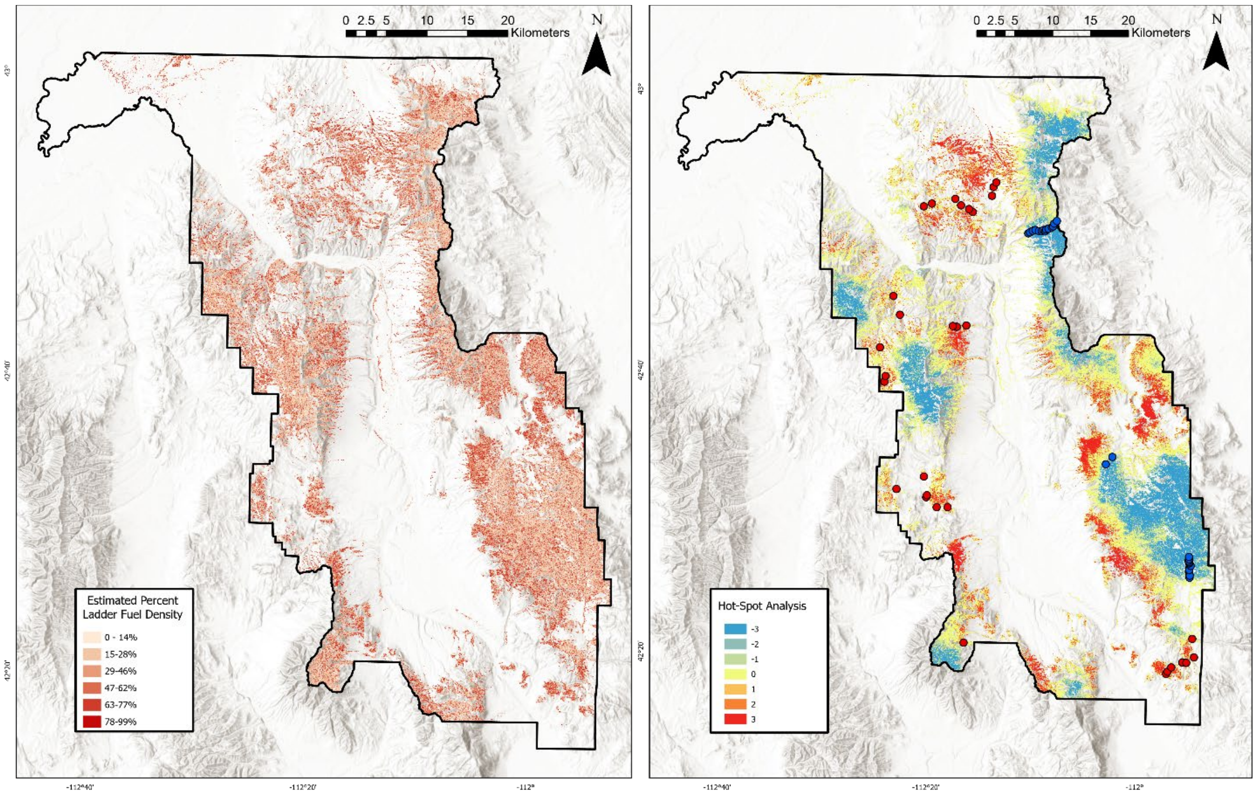

Figure 3. Raster image (1 meter per pixel) depicting the estimated density of ladder fuels in the forested regions in Bannock County (left). Raster image (1 meter per pixel) depicting the results of the Getis-Ord hot spot analysis with the study POIs overlaid (right)

RESULTS AND DISCUSSION

Validation of the LFCM for Bannock County, Idaho used 61 chosen POIs. A total of 248 photographs were taken at these sites along with observations, measurements, and site attributes. Analysis indicated that 56% of sample sites from project areas were collected in 2023 and that 74% of samples sites from only two lidar project areas. The horizontal positional accuracy of sample points derived using the default GNSS receiver onboard the Apple iPhone 14 was assumed to be +/- 5 [30]. This level of positional accuracy ensures the actual sample point most likely falls somewhere within the 20 meters buffer polygon used for analysis. The mean tree height at the sample sites was 15 meters. In both low and high percent ladder fuel sites, broadleaf forests were slightly more common. Of the POIs with low estimated ladder fuel density (**Figure 4**), 30% had a conifer dominated over story and 70% had broadleaf dominated over story.

Of the POIs with high estimated ladder fuel density (**Figure 5**), 42% had a coniferous dominated over story and 58% had broad leaf dominated over story. All POIs visited had some degree of ladder fuel present which agreed well with predictions from the LFCM. The in-situ ladder fuel abundance observations gathered suggest that the LFCM correctly estimated actual ladder fuel conditions observed in the field. Based upon the LFCM, the minimum and maximum percent ladder fuel density at low ladder fuel field sites was 16.5% and 39.9%, and the minimum and maximum percent ladder fuel density values at estimated high ladder fuel density sites was 27.7% to 70.4% (**Table 6**).

Figure 4. A point of interest with low estimated ladder fuel density. The estimated ladder fuel density for this POI is 21.4%

Figure 5. A point of interest with high estimated ladder fuel density. The estimated ladder fuel density for this POI is 58.0%

The values for mean and standard deviation were used to calculate a 95% confidence interval for each of the two ladder fuel classes. This analysis indicated that 95% of low ladder fuel density sites could be expected to exhibit between 20.2–39.8% ladder fuel density, while 95% of high ladder fuel density sites could be expected to exhibit between 28.3-63.9% ladder fuel density.

Table 6. Summary statistics for the mean estimated ladder fuel density percent value for study POIs. POIs were chosen using a Getis-Ord hot spot analysis which identified particular areas of interest having very high or very low ladder fuel density estimates.

Point of Interest	*n* =	Min (%)	Max (%)	Mean (%)	St. Dev
Low	30	16.5	39.9	30.0	5.0
High	31	27.7	70.4	46.1	9.1

A two-sample T-test and Analysis of Variance was used to statistical analyze the ladder fuel validation data, see **Figure 6**. The results suggest the low and high ladder fuel density sites are significantly different ($P < 0.001$) and correspond well with field validation observations. These results indicate that sites with estimated low ladder fuel density do indeed exhibit low ladder fuel abundance, and sites with estimated high ladder fuel density do indeed exhibit high ladder fuel abundance. The statistically derived confidence interval along with the minimum, maximum, and mean values demonstrate that the LFCM can accurately demarcate between low and high ladder fuel sites.

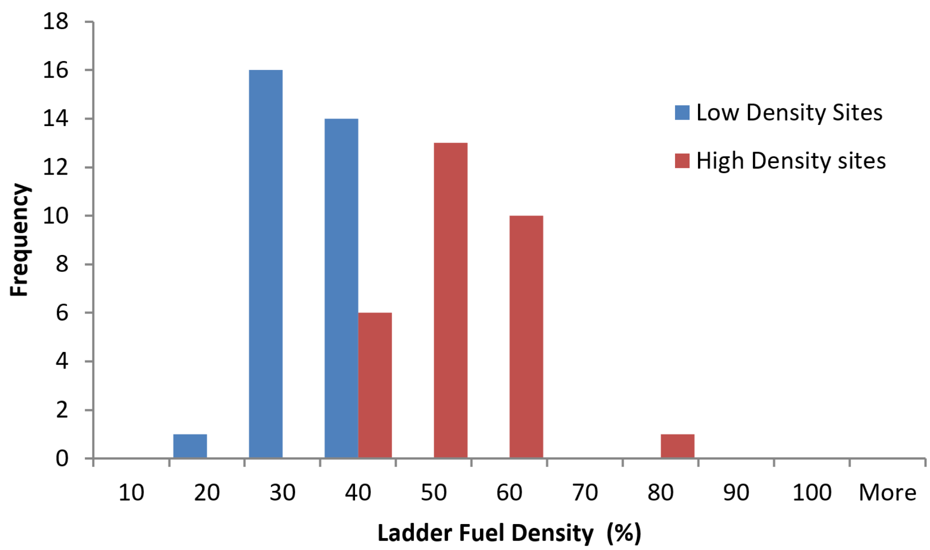

Figure 6. Results from a two-sample T-test and analysis of variance (ANOVA) indicate that low and high ladder fuel density sites are significantly different ($P < 0.001$) and correspond well with field validation observations.

Ideally, the Bannock County study area LPC data would have been collected and delivered very shortly before the 2025 summer field season commenced. However, this was not the case and, as is common with lidar data collections, complete coverage for the entire study area was accomplished through several projects. It is possible that changes in the study area occurred between the time the lidar collection was made and study took place; however, no known large disturbances occurred at any of the sample sites that we are aware of. Furthermore, all lidar collections were either QL2 or QL1 and followed the current USGS lidar specifications.

While the LFCM applies height normalization procedures to input LPC data, no point intensity normalization procedures were included in the model. Point intensity normalization features could be beneficial however in addressing data issues caused by heterogeneous point densities that result from the use of multiple input LPC sources. To mitigate the negative effects of this, it is recommended that users of the LFCM limit input LPC data to the most current lidar project dataset whenever possible. To improve the functionality of the model, we plan to add LPC intensity normalization procedures to future iterations of the LFCM.

The forest types present in Bannock County are comparable to the forest types present in the study area used in Kramer's [11]. research. However, Kramer's equation has limited applicability over varying forest types. The accuracy of the LFCM, when completed for Bannock county, could potentially have been improved upon if the metrics derived in step 2 of the model were tuned specially for Bannock County's fire regime. We suggest that users of the LFCM alter the metrics derived in step 2 of the model to more closely align with their local fire regimes.

A directed sampling approach was used during the validation of the LFCM. This approach was chosen due over a single or double-blind approach to logistical and time constraints for the summer field season. The majority of the study area contained only moderate ladder fuel density forests, and because of this a randomized sampling method presents the potential for an insufficient quantity of low or high ladder fuel sites to be visited. Because sites with especially high ladder fuel densities are of peak interest, this would result in the applicability of this model for actual wildfire mitigation being unknown. In other words, it was crucial that both low ladder fuel sites and high ladder fuel sites were visited and validated. It is of note that only one technician was present during model validation efforts. This increases the potential for individual observation bias or human error in validation observations. This particular field validation approach was purposely chosen to determine if high-density ladder fuel areas could be identified and distinguished from low-density ladder fuel areas. Adding a third category of field observation (moderate-density ladder fuels) was considered, however a problem arose in the reliability of the field observer's ability to properly quantify moderate-density ladder fuel areas. The potential for errors in field observation uncertainty were great enough that this category was eliminated prior to the field season. As a result, focus was placed on determining if high-density ladder fuel areas could be differentiated from low-density sites to aid land managers with wildfire fuel load reduction treatment prioritization.

Overall, our findings suggest the LFCM can be used to differentiate areas with varying ladder fuel densities. More importantly, our findings suggest the model can be used to identify forested areas with high ladder fuel density. In turn, these areas can be reliably delineated for application of priority fuel load reduction treatments. The LFCM eliminates the need for ladder fuel hazard assessments to be conducted manually. This reduces the amount of manpower needed, making the assessment process faster and cheaper. The LFCM minimizes the amount of human involvement needed to perform the ladder fuel hazard assessment calculations which minimizes operator error and streamlines the assessment process.

CONCLUSIONS

We developed a freely available model and associated tutorial documentation that allows a user to create a ladder fuel density raster layer for any forested AOI. This model follows a methodology that has been used for ladder fuel cover estimation with measurable success in the past. Field validation (n = 61) indicates the model can accurately identify areas with low ladder fuel density (20-40%) and reliably discriminate these sites from areas with high ladder fuel density (28-64%). While there is some overlap between low density and high-density confidence intervals, the LFCM can be used effectively to help identify areas to prioritize for wildfire fuel reduction treatments and fire mitigation. Although the LFCM has not been tested across all possible forest type scenarios, the model provides a valuable tool for establishing a strong baseline for priority hazardous fuel reduction treatment delineation. We encourage continued research of lidar applications for environmental conservation and land management. Additionally, we encourage others to further explore the functionality and accuracy of the LFCM.

Author Contributions: Conceptualization, H.C. and K.W.; methodology, H.C.; software, H.C.; validation, H.C., K.W.; formal analysis, K.W.; investigation, H.C.; resources, H.C.; data curation, H.C.; writing---original draft preparation, H.C.; writing---review and editing, H.C.; visualization, H.C.; supervision, K.W.; project administration, K.W.; funding acquisition, H.C.

Funding: This work was made possible by a grant from the United States Department of Homeland Security, Federal Emergency Management Agency (FEMA), Cooperating Technical Partners (CTP) program (EMS-2023-CA-05002 and EMS-2024-CA-05000).

Data availability: The original data presented in the study are openly available at: https://giscenter.isu.edu/research/Techpg/FEMA_DOS/zip/LF_Model_Current.zip

Acknowledgements: The authors would like to thank Mr. Cole Rosner at Idaho State University's GIS Training and Research Center who assisted with python coding. The authors have reviewed and edited the output and take full responsibility for the content of this manuscript.

Conflict of Interest: The authors declare no conflicts of interest.

REFERENCES

1. Jones, M.W.; Smith, A.; Betts, R.; Canadell, J.G.; Prentice, I.C.; Le Quéré, C. Climate change increases the risk of wildfires. ScienceBrief 2020.
2. Weber, K.T.; Yadav, R. Spatiotemporal trends in wildfires across the Western United States (1950–2019). Remote Sensing 2020, 12, 2959. https://doi.org/10.3390/rs12182959.

3. Zou, Y.; Rasch, P.J.; Wang, H.; Xie, Z.; Zhang, R. Increasing large wildfires over the western United States linked to diminishing sea ice in the Arctic. Nature communications 2021, 12, 6048. https://doi.org/10.1038/s41467-021-26232-9.

4. Hessburg, P.F.; Agee, J.K.; Franklin, J.F. Dry forests and wildland fires of the inland Northwest USA: contrasting the landscape ecology of the pre-settlement and modern eras. Forest Ecology and management 2005, 211, 117–139. https://doi.org/10.1016/j.foreco.2005.02.016.

5. Hakkenberg, C.R.; Clark, M.L.; Bailey, T.; Goetz, S.J. Ladder fuels rather than canopy volumes consistently predict wildfire severity even in extreme topographic-weather conditions. Communications Earth & Environment 2024, 5. https://doi.org/10.1038/s43247-024-01893-8.
326

6. Menning, K.M.; Stephens, S.L. Fire climbing in the forest: a semiqualitative, semiquantitative approach to assessing ladder fuel hazards. Western Journal of Applied Forestry 2007, 22, 88–93. https://doi.org/10.1093/wjaf/22.2.88.

7. Pye, J.M.; Prestemon, J.P.; Butry, D.T.; Abt, K.L. Prescribed Burning and Wildfire Risk in the 1998 Fire Season in Florida. In Proceedings of the Proceedings of the USDA Forest Service Proceedings RMRS-P-29, Research Triangle Park, NC, USA, 2003; pp. 15–26.

8. Alonso-Rego, C.; Fernandes, P.; Álvarez-González, J.G.; Arellano-Pérez, S.; Ruiz-González, A.D. Individual-Tree and Stand-Level Models for Estimating Ladder Fuel Biomass Fractions in Unpruned Pinus radiata Plantations. Forests 2022, 13, 1697. https://doi.org/10.3390/f13101697.

9. Campbell, M.J.; Dennison, P.E.; Hudak, A.T.; Parham, L.M.; Butler, B.W. Quantifying understory vegetation density using small-footprint airborne lidar. Remote sensing of environment 2018, 215, 330–342. https://doi.org/10.1016/j.rse.2018.06.023.

10. Kramer, H.A.; Collins, B.M.; Kelly, M.; Stephens, S.L. Quantifying ladder fuels: A new approach using LiDAR. Forests 2014, 5, 1432–1453. https://doi.org/10.3390/f5061432.

11. Kramer, H.A.; Collins, B.M.; Lake, F.K.; Jakubowski, M.K.; Stephens, S.L.; Kelly, M. Estimating ladder fuels: a new approach combining field photography with LiDAR. Remote Sensing 2016, 8, 766. https://doi.org/10.3390/rs8090766.

12. Kwok, V. Deriving LiDAR Metrics to Estimate Ladder Fuel Density. https://storymaps.arcgis.com/stories/f6b67be78e134a1e866127f0802b2700, 2024. Accessed: November 18, 2025.

13. Isenburg, M. LAStools: Efficient Tools for LiDAR Processing. Version 2.0.3, 2024.

14. Environmental Systems Research Institute (ESRI). ArcGIS Suite, 2024.

15. Irwin, J.R. Quantification of Understory Fuels in the Superior National Forest Using Lidar Data. Master's thesis, South Dakota State University, Brookings, SD, 2018.

16. Mutlu, M.; Popescu, S.C.; Stripling, C.; Spencer, T. Mapping surface fuel models using lidar and multispectral data fusion for fire behavior. Remote Sensing of Environment 2008, 112, 274–285. https://doi.org/10.1016/j.rse.2007.05.005.

17. LANDFIRE. LANDFIRE Existing Vegetation Type, 2023.

18. Vershum, K.; Latta, G. Bannock County Forest Inventory Stocks. Technical report, University of Idaho, 2022. County-level Forest inventory report.

19. Idaho State Tax Commission. County [Feature layer]. Published by Idaho State Tax Commission on ArcGIS Hub, 2016.

20. Aero-Graphics, Inc. Oxford Slough Waterfowl Production Area LiDAR Data Collection. LAS format v1.2, 2013.

21. Quantum Spatial. Blackfoot & Portneuf, Idaho Lidar Point Cloud Collection. LAZ format, 2018.

22. Quantum Spatial. Franklin Bear, Idaho USGS 3DEP LiDAR. LAS format v1.4, 2018.

23. Quantum Spatial. OLC Snake River FEMA LiDAR Point Cloud Collection. LAZ format, 2016.

24. U.S. Geological Survey, National Geospatial Technical Operations Center. USGS Lidar Point Cloud Collection ID_SouthernID_17_2018. LAZ format, 2023.

25. U.S. Geological Survey, National Geospatial Technical Operations Center. USGS Lidar Point Cloud Collection ID_SouthernID_22_2018. LAZ format, 2023. Version February 11, 2026 submitted to Fire 14 of 14

26. U.S. Geological Survey, National Geospatial Technical Operations Center. USGS Lidar Point Cloud Collection ID_SouthernID_6_2018. LAZ format, 2022.

27. U.S. Geological Survey. USGS Lidar Point Cloud Collection ID_SouthernID_2018. LAZ format, 2023.

28. U.S. Geological Survey, National Geospatial Technical Operations Center. USGS Lidar Point Cloud Collection ID_SouthernID_9_2018. LAZ format, 2023.

29. Getis, A.; Ord, J.K. The Analysis of Spatial Association by Use of Distance Statistics. Geographical Analysis 1992, 24, 189–206. https://doi.org/10.1111/j.1538-4632.1992.tb00261.x.

30. Tomaštík Jr, J.; Tomaštík Sr, J.; Salo ˇn, Š.; Piroh, R. Horizontal accuracy and applicability of smartphone GNSS positioning in forests. Forestry: An International Journal of Forest Research 2017, 90, 187–198. https://doi.org/10.1093/forestry/cpw031.